

LASER INTERFEROMETER GRAVITATIONAL WAVE OBSERVATORY
- LIGO -
CALIFORNIA INSTITUTE OF TECHNOLOGY
MASSACHUSETTS INSTITUTE OF TECHNOLOGY

Document Type LIGO-G950061-02- R 8/29/95

**A Summary and Future Preview of
the FFT Simulation Initiative in LIGO**

Brett Bochner

California Institute of Technology
LIGO Project - MS 51-33
Pasadena CA 91125
Phone (818) 395-2129
Fax (818) 304-9834
E-mail: info@ligo.caltech.edu

Massachusetts Institute of Technology
LIGO Project - MS 20B-145
Cambridge, MA 01239
Phone (617) 253-4824
Fax (617) 253-7014
E-mail: info@ligo.mit.edu

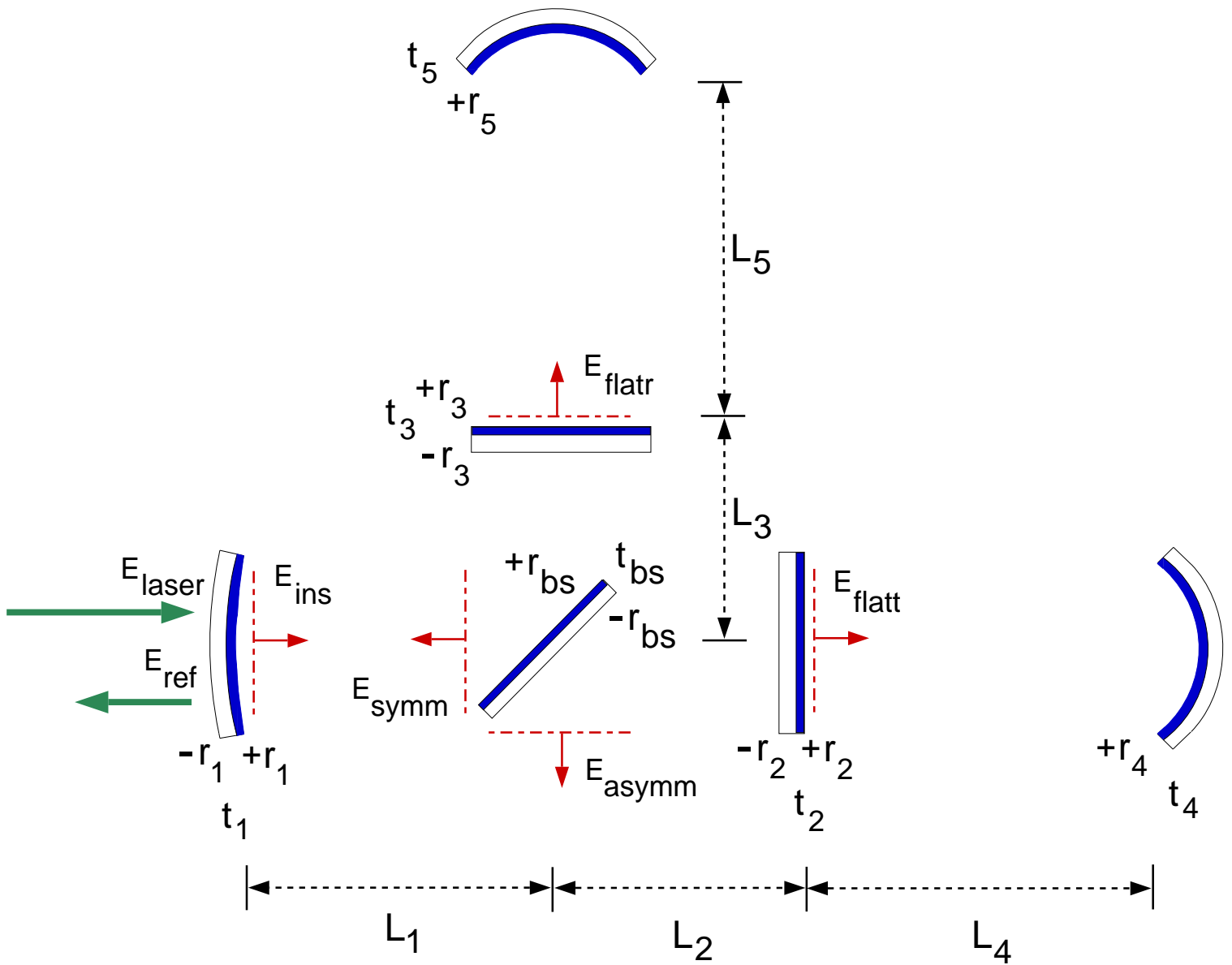
WWW: <http://www.ligo.caltech.edu/>

The FFT Simulation Program Described in a Nutshell

The program created by MIT's "FFT initiative" is a model of the complete 1st-Generation LIGO interferometer: a Recycled Michelson ifo with Fabry-Perot cavity arms and a Schnupp Asymmetry length in the Recycling cavity.

- The model is pseudo-one-dimensional, in that:
 - ›› Propagation is performed via FFT transform methods, using the *Paraxial Approximation*, and:
 - ›› The electric field information is stored as a series of (2-D) transverse slices at various locations in the beam path.
- The model is static, and the outputs are the steady-state fields and field powers at all desired locations in the interferometer.
- The model is resonant, since all lengths and/or frequencies are adjusted to maintain the resonance conditions that maximize the gravity-wave sensitivity.
- The model is (nearly-)complete, in that both the Carrier and its Signal-Sideband fields can be simulated (usually 1 of the 2 Sidebands is), to produce the full shot-noise-limited sensitivity, $h(f)$. (But the effects of the Subcarrier & its sidebands are not modelled.)
- The model is optimized in 3 additional ways: (i) The Recycling Mirror Reflectivity is adjusted to maximize the Carrier power everywhere, (ii) the Schnupp Asymmetry is adjusted to maximize transmission of Sideband power out of the antisymmetric port of the beamsplitter, and: (iii) The Sideband Modulation Depth is chosen in post-processing to optimize $h(f)$.
- The model is realistic, in that it includes: (i) Realistically-deformed optics, (ii) Mirror tilts & beam mismatch, (iii) Finite Apertures, and: (iv) Power Losses (Absorptive+Scattering).

Diagram of a Full-LIGO Interferometer



Physical Input Parameters for Program :

Physical Parameters Calculated By Program :

- 1) Wavelength of laser.
- 2) Spatial mode shape of laser beam (TEM_{00}).
- 3) Macroscopic Distances $L_1 - L_5$.
- 4) Radii of curvature of FP back mirrors.
- 5) Reflectivities of mirrors.
- 6) Losses in mirrors.
- 7) Diaphragms of mirrors.
- 8) Mirror tilts.
- 9) Mirror displacements (transverse to beam).
- 10) Mirror base thicknesses (in wavelengths).
- 11) Mirror surface & substrate imperfections.
- 12) Transverse offset of laser beam.
- 13) Size of square calculational window.

- 1) Waist size of laser beam.
- 2) Radius of curvature of recycling mirror (matched to E_{ins}).
- 3) Microscopic adjustments to L_2, L_3, L_4, L_5 .
- 4) Steady-state fields $E_{ins}, E_{ref}, E_{flatt}, E_{flatr}, E_{symm}, E_{asymm}$.

A Brief History of LIGO's FFT Simulation Initiative

July '92 and Earlier : **J. Y. Vinet, P. Hello, C. N. Man, & A. Brillet of VIRGO**

Creation of program. Configuration: An unrecycled Michelson interferometer with Fabry-Perot arms.

Steady but very slow field-relaxation convergence.

Mirror imperfections could include zernikes, randomized roughness, tilts & finite apertures.

Mid '92 --> Mid '93, Beginning of LIGO work : **Yaron Hefetz & Partha Saha**

Configuration: Recycling mirror added, an FP arm absent or "perfect". Essentially a 3-mirror double cavity.

Development of *rapid* ("Smart") convergence method, many-fold improvement in program speed.

Use of (slow) two-dimensional search for simultaneous optimization of the 2 cavity lengths.

Work done with mirror tilts and zernike mirror deformations.

Mid '93 --> Early '95 : **Yaron Hefetz & Brett Bochner**

Configuration: The "full-LIGO", i.e. a Recycled Michelson ifo with FP arms & a Schnupp length asymmetry.

Use of faster length adjustment methods, using phase comparisons between fields propagated around the ifo.

Creation & introduction of Realistic Mirror Maps for mirror surface & substrate deformations.

Simulation of Signal-Sideband as well as Carrier fields, to calculate the shot-noise-limited $h(f)$.

First major services done for the LIGO project with the FFT simulation program.

Early '95--> Now (Mid '95) : **Brett Bochner**

Introduction of a beamsplitter with realistic deformations & a finite aperture.

Gridding studies & simple anti-aliasing procedures.

Into the Future . . . ? : **Brett Bochner & Hiro Yamamoto (& Others?)**

Brett: Thesis work, primarily the study of a Dual-Recycled LIGO interferometer (begun in Summer '95).

Hiro (& Others): Simulations for the System Integration modeling effort, & other simulations upon request.



Tests of the Realism and Accuracy of the FFT Program

We have taken steps to prove that results from the FFT simulation program can be regarded as physically accurate and complete. This has included careful examinations of the results to check that they make intuitive sense, and well as comparisons of the simulation output results with results obtained with other approaches. Some of these comparisons and checks are as follows:

1. Comparisons of FFT results with those in the literature¹ for the round-trip losses of the lowest eigenfield of a symmetric cavity with Perfectly Smooth & Reflective but Finite-Aperture mirrors. (Figures follow.)
2. Comparisons with the Mathematica-based “Modal Model”² for a full-LIGO-configuration run with tilted front & back arm cavity mirrors. (Table of data follows.)
3. Comparisons with analytical calculations³ of the power stored in a (simple) cavity with Zernike Polynomial deformations on the mirrors, and of the interference fringe of the cavity-reflected field with a perfect TEM00 field. (Table of data follows.)
4. Mathematical estimations of the adequacy of the gridding, and comparisons with double-pixel (256x256) runs, which have either double the calculational window size or double the pixel density. (Calculations follow.)

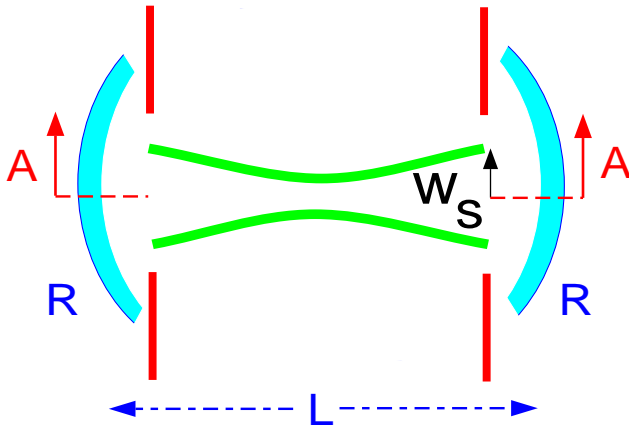
1. T. Li, Bell Syst. Tech. J. **44**, 917 (1965); H. P. Kortz and H. Weber, Appl. Opt. **20**, 1936 (1981).

2. Model by Yaron Hefetz & Nergis Mavalvala.

3. Calculations by P. Saha, Y. Hefetz & R. Weiss.

FFT Test #1: Comparison with Published Diffraction-Loss Results

The System:



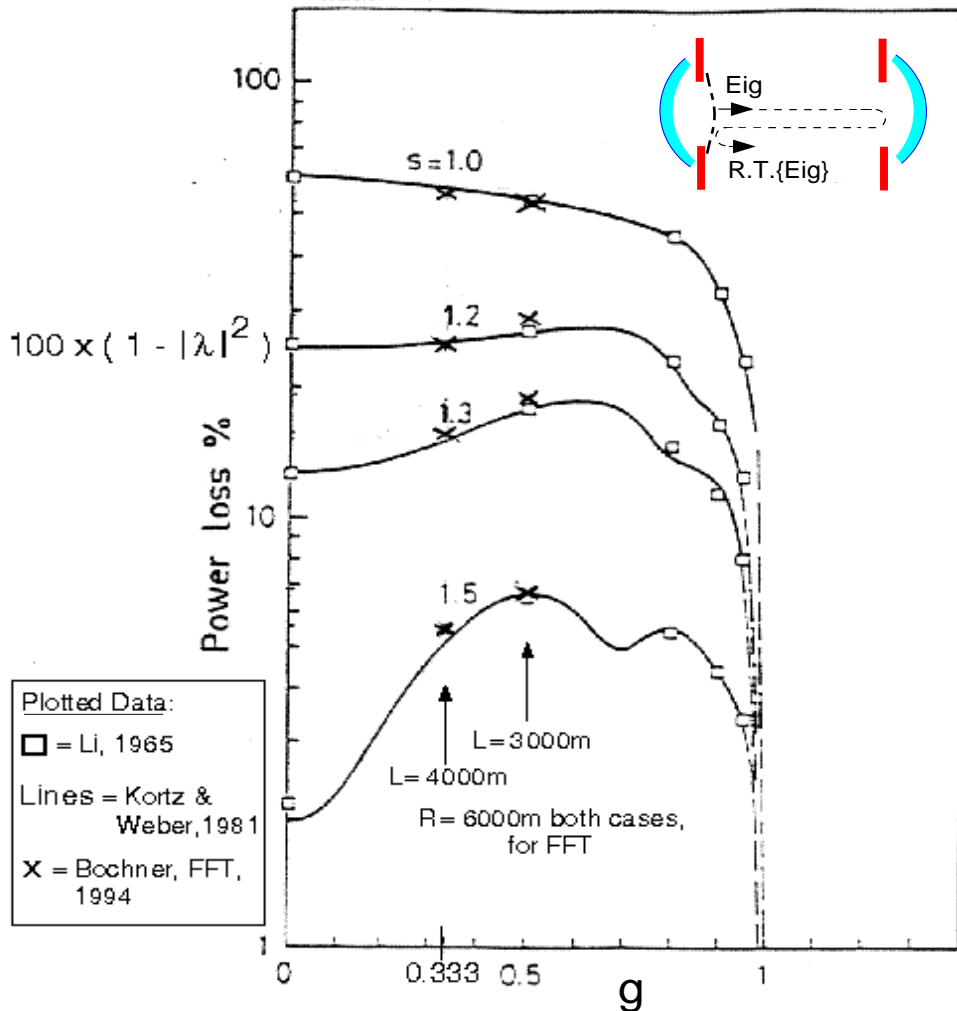
The Formulae:

$$g = 1 - L/R$$

$$w_s = \frac{\lambda L}{\pi} (1 - g^2)^{-1/2}$$

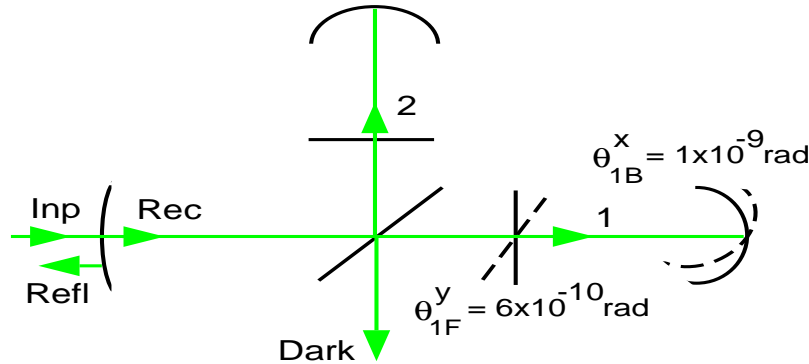
$$S = A/w_s$$

Comparison of the three data sets:



Power loss per full resonator round trip for the two-aperture case for four different adapting factors of the aperture size to the Gaussian beam size.

FFT Test #2: Comparing FFT Results with the Modal Model for Tilts of the FP Arm Cavity Mirrors



Carrier	TEM00	TEM10	TEM01
Field Position:			
1 (FFT)	2462.26	1.89859e-4	2.27572e-5
1 (M.M.)	2462.26	1.89859e-4	2.27572e-5
2 (FFT)	2462.26	4.23609e-9	3.25929e-10
2 (M.M.)	2462.26	4.23618e-9	3.25904e-10
Rec (FFT)	37.8732	7.44302e-7	5.72611e-8
Rec (M.M.)	37.8732	7.44284e-7	5.72659e-8
Refl (FFT)	9.18050e-5	2.05475e-8	1.55318e-9
Refl (M.M.)	9.18084e-5	2.05469e-8	1.55335e-9
Dark (FFT)	6.403e-14	2.90692e-6	1.14517e-7
Dark (M.M.)	2.241e-12	2.90686e-6	1.14536e-7
Sideband	TEM00	TEM10	TEM01
Field Position:			
1 (FFT)	0.140946	1.12104e-6	2.12684e-7
1 (M.M.)	0.140946	1.09742e-6	2.17620e-7
2 (FFT)	0.140946	8.39382e-7	1.97733e-7
2 (M.M.)	0.140946	8.16650e-7	2.02886e-7
Rec (FFT)	37.1454	7.16416e-5	1.78193e-5
Rec (M.M.)	37.1455	7.17492e-5	1.78251e-5
Refl (FFT)	1.11418e-7	1.98492e-6	4.92624e-7
Refl (M.M.)	8.88168e-8	1.98365e-6	4.92794e-7
Dark (FFT)	0.985081	1.93300e-6	1.01603e-7
Dark (M.M.)	0.985082	1.92905e-6	1.01376e-7

FFT Test #3: Comparisons with Analytical Calculations for a Single Fabry-Perot Cavity with Zernike Polynomial Mirror Deformations

The System: One Fabry-Perot cavity with a $\lambda/300$ zernike surface deformation upon either the front mirror or the back mirror. Interference of the cavity reflected field with the field from an “ideal” cavity at an “ideal” beamsplitter.

The Methods: Numerical: An early version of the FFT program. (Implemented by P. Saha.) Analytical: A perturbation expansion to find the resonant power in the fundamental eigenmode of the deformed cavity. (By R. Weiss & P. Saha.)

The Definitions:

$$\alpha = 1 - \frac{\text{Power}_{\text{perturbed-cavity}}}{\text{Power}_{\text{perfect-cavity}}} , \quad (1 - \text{Contrast}) \approx 2 \cdot \frac{\text{Power}_{\text{splitter-dark}}}{\text{Power}_{\text{splitter-bright}}}$$

The Results: Front Mirror Perturbations

Zernike (n,l)	1-Contrast		α	
	numerical	analytical	numerical	analytical
(5,1)	1.36e-4	1.35e-4	1.64e-4	1.68e-4
(6,0)	2.54e-5	2.60e-5	4.01e-5	7.71e-5
(7,1)	4.02e-4	4.10e-4	4.05e-5	3.79e-4
(8,0)	9.39e-5	9.74e-5	1.99e-4	1.17e-4
(9,1)	1.01e-3	9.80e-4	8.77e-4	7.70e-4

The Results: Back Mirror Perturbations

Zernike (n,l)	1-Contrast		α	
	numerical	analytical	numerical	analytical
(5,1)	1.11e-3	1.07e-3	6.14e-4	5.93e-4
(6,0)	4.71e-4	4.54e-4	4.17e-4	2.12e-4
(7,1)	2.18e-3	2.18e-3	1.11e-3	1.76e-3
(8,0)	9.56e-4	9.28e-4	5.65e-4	7.16e-4
(9,1)	2.69e-3	2.63e-3	3.42e-3	3.77e-3



FFT Issue #4: Grid Pixelization, Sampling Adequacy, and Aliasing Considerations

In any calculation representing continuous & infinite information with discrete & finite grids, the grid must significantly represent the continuous field information. This requirement can be expressed as inequalities in two regimes:

1. (Fine x-space sampling) \iff (High-momentum p-space information):

$$\frac{\sqrt{\text{Number of Order Unity}}}{N_{\text{pixels}}} \cdot \frac{2 \cdot \text{Window}}{\pi \cdot \text{Waist}} \ll 1$$

2. (Large x-space window) \iff (Fine p-space sampling):

$$\sqrt{\text{Number of Order Unity}} \cdot \frac{\text{Window}}{\pi \cdot \text{Waist}} \gg 1$$

These inequalities in particular have been derived for TEM00 beams (not just at the waist, but everywhere), and similar relations (perhaps different by small numerical factors) can be derived for the other modes.

Note also that these nearly contradictory inequalities can *both* be true only if the number of pixels in the map, N_{pixels} , is LARGE.

- If inequality #1 is violated, then sampling the TEM00 input laser beam on the grid *aliases* high-“momentum” beam information into low-“momentum” info.
- If inequality #2 is violated, then much power in the beam is cut out and ignored by the small window. In addition, there is the problem of “position-space aliasing” (see next page for details).

For the current parameters of our interferometer simulations:

$N_{\text{pixels}} = 128$, $\text{Window} = 35 \text{ cm}$, $\text{Waist} = 2.15 \text{ cm}$, $\text{Number (“e-foldings”)} \sim 2$,

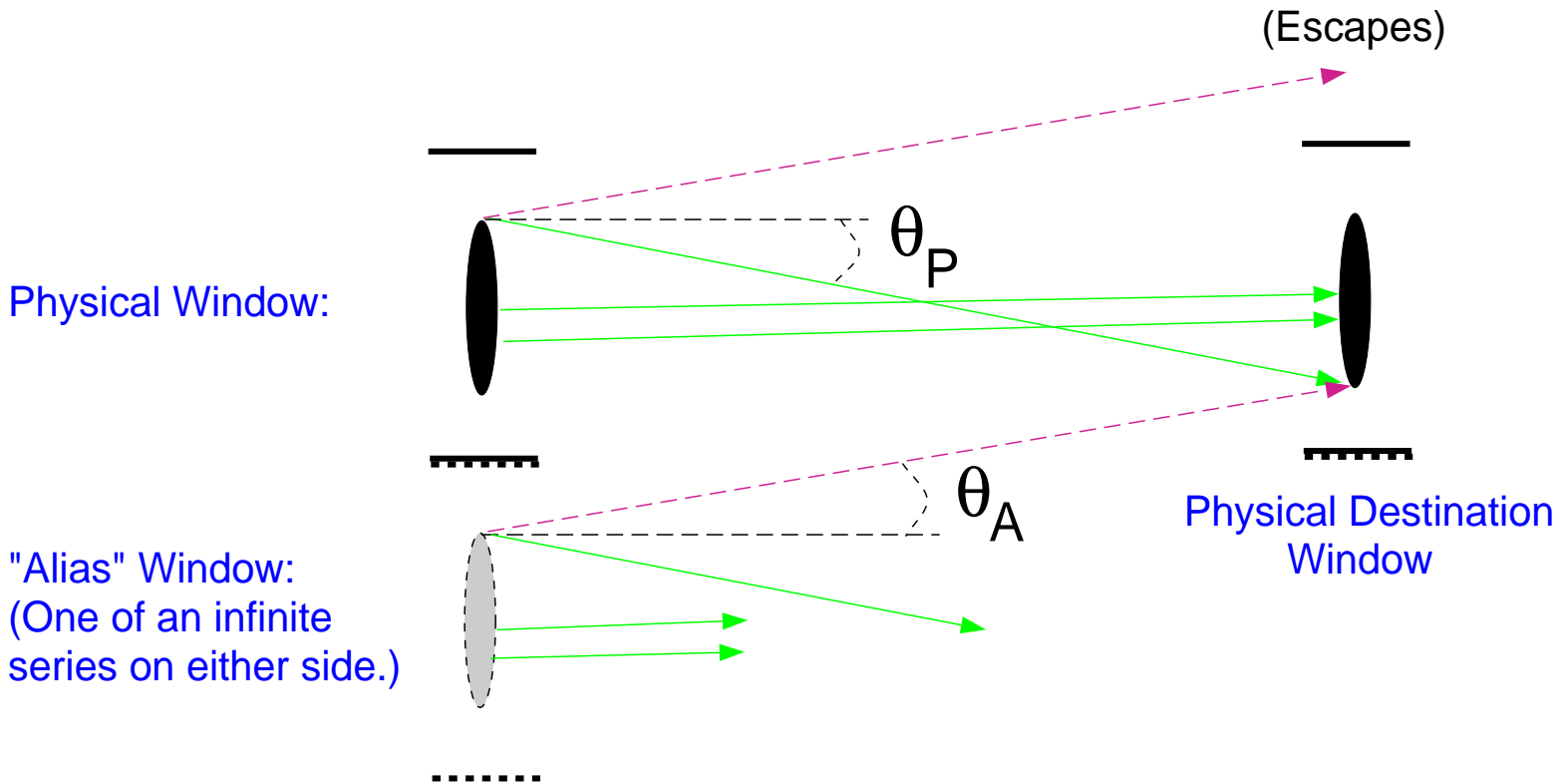
therefore: (Inequality #1) = .123 \sim 1/8 \ll 1, and (Inequality #2) = 7.9 \gg 1 !

\implies The grid & window size parameters are *well chosen* for our beam parameters, insofar as the beam is mostly TEM00 (and other “low”-index modes).

FFT Issue #4, continued: Position-Space Aliasing

A consequence of too-small calculational windows (= too-coarse p-space information) is “position-space aliasing”, which is a result of: **lack of information outside the calculational window that is reinterpreted in Fourier space as repeated information + beam spread during propagation.**

Pictorially, this occurs as follows:



We see that repeated beam information in the “alias” window can travel into the mirror aperture on the real, “physical destination” window.

This effect can be serious if rough mirrors create high-angle scatter in the beam, and if the calculational windows are not much larger than the mirror apertures.

Example: Runs w/different pixelizations, $\lambda/900$ mirror surface & substrate deformations:

No Anti-Aliasing Procedures	128x128 Grid	256x256 Grid (Double-Sized Window)	256x256 Grid (Double Pixel Density)
Carr. Power in FP Arms :	1994.2	2011.7	2090.3
Carrier Contrast Defect :	1.298e-3	7.954e-4	8.241e-4
$h(f) = 1/\text{SNR}(f) @ 100\text{Hz} :$	9.192e-24	8.943e-24	8.787e-24

FFT Issue #4, cont'd: Eliminating Position-Space Aliasing

The solution to this problem of aliasing is to *eliminate as much of the aliased information as possible, while retaining as much of the physically accurate information as possible.*

[As per the diagram on the previous page, we define:](#)

θ_P = The largest angle that physical information can travel at and still enter the mirror aperture at the destination window.

θ_A = The smallest angle that alias information can travel and enter the aperture at the destination window.

In general, we may have either $\theta_P > \theta_A$ or $\theta_P < \theta_A$.

Our solution to aliasing is to cut unwanted information out of the FFT propagator. The cut is done as follows:

$\theta < \theta_A$: No change to these propagator pixels.

$\theta_P > \theta > \theta_A$ (The *Overlap Region*, if it exists): Utilize some apodization function that gradually eliminates information information at higher angles.

$\theta_{\text{max-on-grid}} > \theta > \theta_P$: Zero-out these propagator pixels.

Only the arm-cavity propagators have a small enough θ_A (compared to $\theta_{\text{max-on-grid}}$) to have information cut out of them, for the normal-sized window runs -- and **no propagator need be altered for the double-sized window runs.**

[Example:](#) Same deformed mirror runs as before, but now using our solution:

New Anti-Aliasing Procedures	128x128 Grid	256x256 Grid (Double-Sized Window)	256x256 Grid (Double Pixel Density)
Carr. Power in FP Arms :	2011.3	2011.7	2071.7
Carrier Contrast Defect :	7.944e-4	7.954e-4	7.814e-4
$h(f) = 1/\text{SNR}(f)$ @ 100Hz :	8.944e-24	8.943e-24	8.802e-24

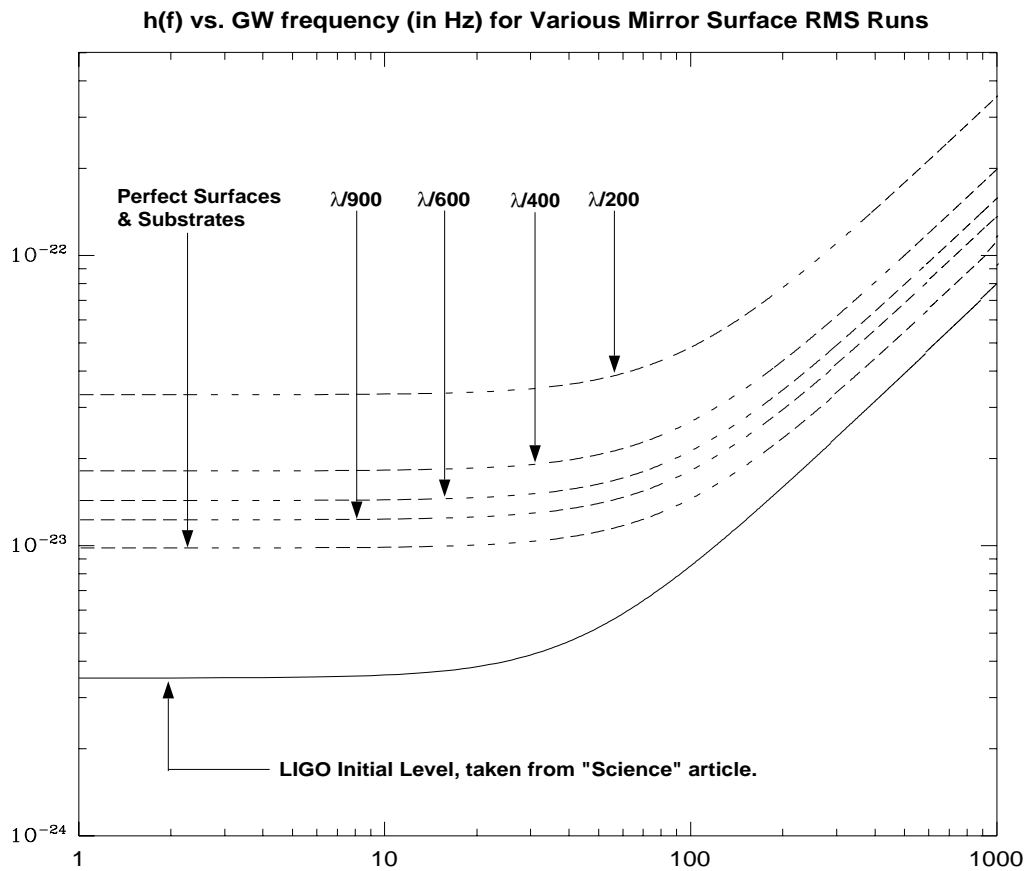
The agreement between the three runs is significantly better than before!

This method of eliminating “position-space” aliasing should work without flaw, as long as the mirrors are not dominated by deformations in the “overlap region”.

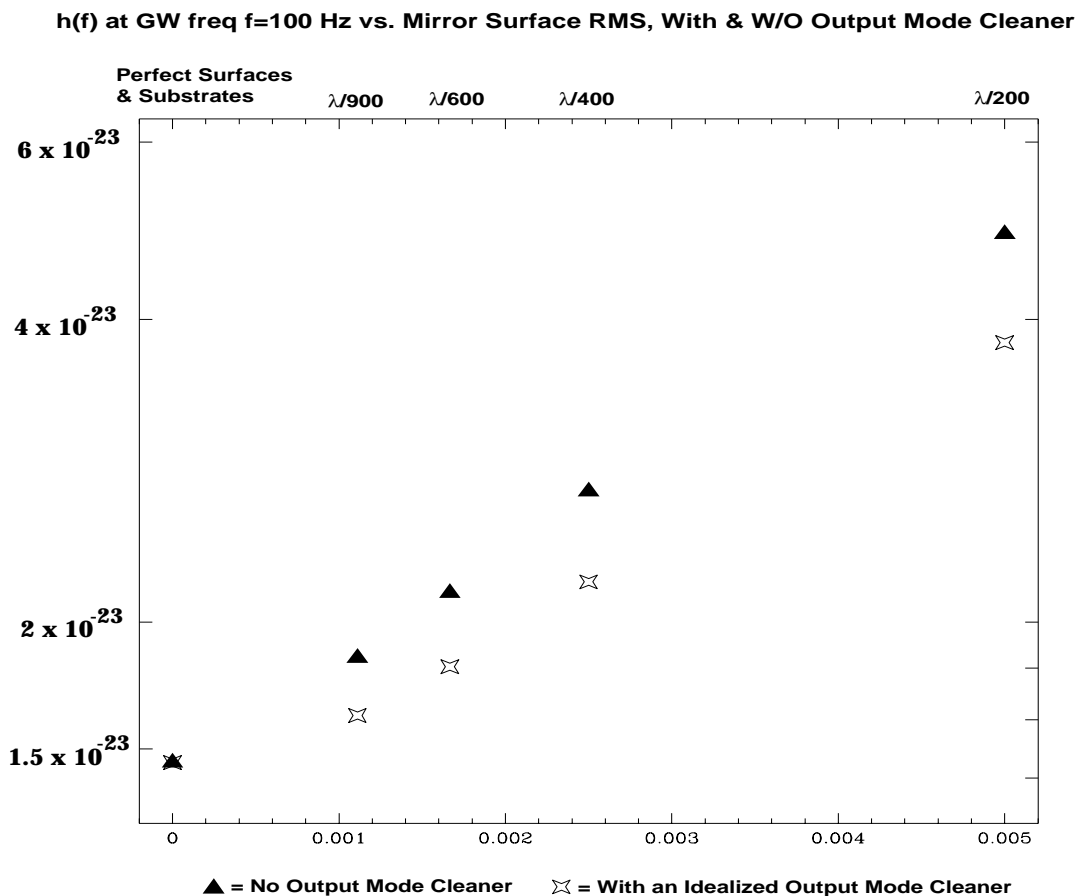
How FFT Simulation Work has Supported Detector and R&D Efforts

1. FFT simulations helped show that mirror figure errors were not significantly more problematical with the Schnupp Asymmetry signal readout scheme than with the Mach-Zehnder scheme.
2. As part of the Pathfinder Project, FFT results helped determine the specifications for the rms deviations of the mirror surfaces.
3. A sample run with a “Realistic” Beamsplitter (& typically deformed mirrors) indicates that the interferometer sensitivity & contrast defect are not significantly degraded by beamsplitter imperfections.
4. FFT runs with a laser wavelength of 1.06 microns (Nd:YAG), have shown that running with the larger wavelength is quite feasible with the standard LIGO configuration & optical parameters.
5. FFT simulations have assisted in the design of the Fixed-Mass Interferometer for the Auto-Alignment experiment at MIT, by predicting the amount of unwanted light modes which may confuse the alignment control systems.
6. Decompositions of the FFT-simulated output fields indicates that even an “ideal” Output Mode Cleaner should only improve $h(f)$ by ~10-20% (although the contrast defect is greatly improved).

Some Plots From the Runs for the Pathfinder Project

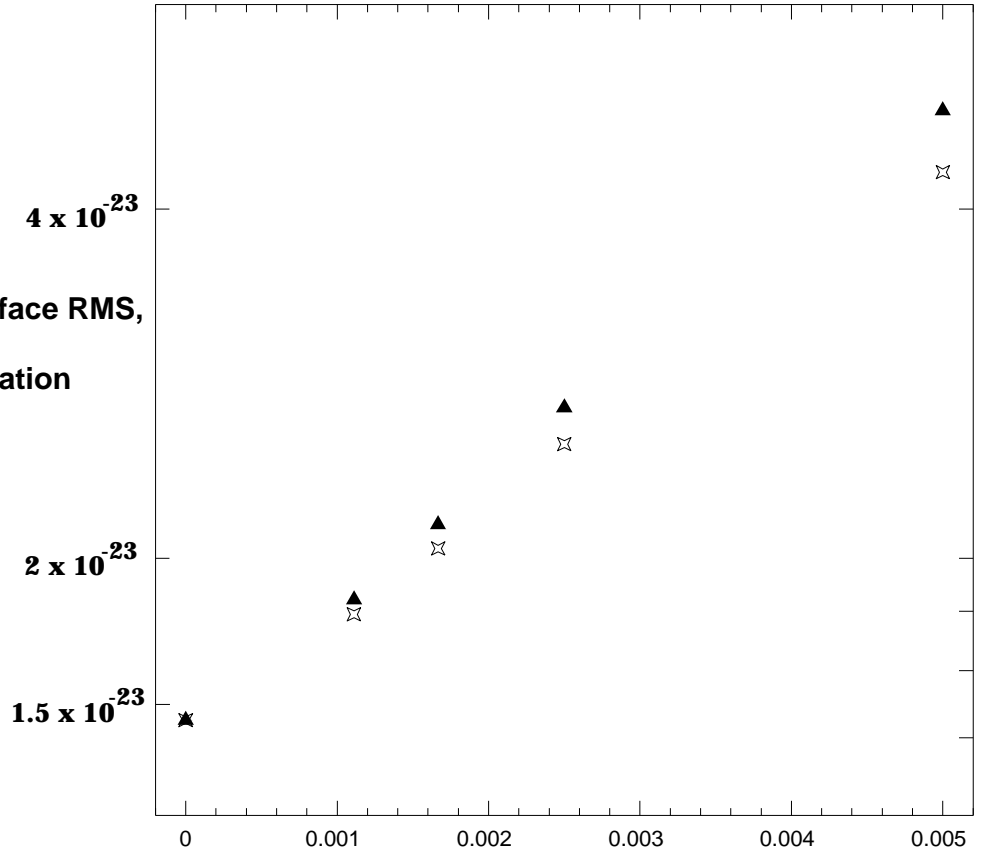


(Note: These results were obtained by the FFT program before the anti-aliasing methods were introduced.)



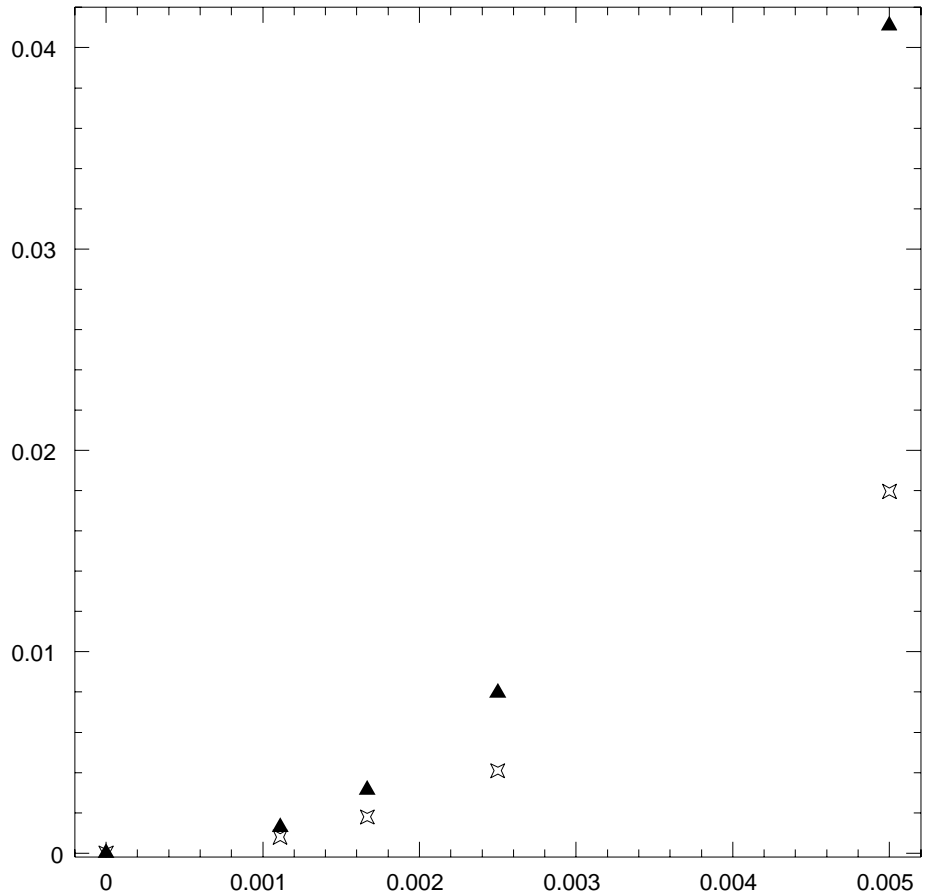
Re-done Pathfinder Results with Anti-Aliased Propagators

**h(f) at GW freq f=100 Hz vs. Mirror Surface RMS,
Before & After FFT Propagator Apodization**



▲ = Original Pathfinder Runs; No Apodization. ✕ = New Results, With Propagator Apodization.

**Contrast Defect vs. Mirror Surface RMS,
Before & After Propagator Apodization**



▲ = Original Pathfinder Runs; No Apodization. ✕ = New Results, With Propagator Apodization.

How FFT Work Can Support “Initial”-LIGO Design in the Future:

Many important questions and situations can be well addressed with the FFT simulation program and its auxiliary programs (e.g. modal decomposition, etc.).

Some interesting examples are:

1. Simulating the performance of half-length (2-km arm) interferometers.
2. Calculating the LIGO gravity-wave sensitivity with maps of the mirrors purchased by the project, when they are received. Further calculations may be done with maps of the mirrors after they are given reflective & a.r. coatings.
3. Providing further assistance in studying the possible move from Argon-ion lasers at 514nm to Nd:YAG lasers at 1.06 microns.
4. Calculating how smaller-scale (~1.5 mm or less) mirror defects degrade the sensitivity.
5. Quantifying the effects of using a spatially-imperfect or displaced input laser beam, to help place limits upon the performance of the Input Mode Cleaner.
6. Quantifying the effects of imperfect mirrors, tilts, & mismatch upon the control signals that lock the cavity lengths and perform angular alignment.
7. Quantifying the effects of variations in the *magnitude* of R and T across a coated mirror surface upon the gravity-wave sensitivity.
8. Helping fix the parameters of the 1st-Generation LIGO ifo's. Some parameters that may be studied: arm cavity g-factors, and the reflectivities of the power-recycling mirror and the arm-cavity input mirrors.
9. Modeling interferometers with curved FP-arm input mirrors and strong-focusing optics to break the degeneracy in the Recycling cavity.

Alternate Configurations: FFT Simulation of Dual-Recycling

In addition to aiding with the future LIGO Detector efforts, FFT Simulation techniques can be useful in creating a quantitative understanding of advanced LIGO designs, such as *Dual Recycling*, in which a “Signal-Recycling” mirror is placed after the antisymmetric port of the beamsplitter to form a cavity (SRC).

What Dual Recycling (Supposedly) Does:

- Resonantly amplifies the gravity-wave-induced signal field in the SRC, and:
- Increases the stored carrier power in the ifo & reduces noise from poor carrier contrast at the beamsplitter, via “mode healing” of the dual-recycled Carrier light.

Some Questions of Interest:

1. Does “mode healing” really exist, i.e. the recycling of discarded carrier light at the beamsplitter back into useful TEM00 light in the interferometer?
2. Is Dual-Recycling really more tolerant to mirror deformations, misalignments & mismatch than the 1st-Generation LIGO design of Power Recycling only?
3. Can a narrowbanded Signal Recycling cavity, tuned to a particular signal frequency, amplify the gravity-wave signal greatly despite imperfect mirrors?
4. Will FP arm cavities, realistically-deformed optics, and LIGO-like dimensions lead to unexpected answers to these questions?

Will only plan on a primitive model for now:

- Carrier simulation only; no Sidebands for control systems or quantitative predictions of degradation to $h(f)$ due to realistic mirror effects on Sidebands.
- Gravity-wave sensitivities estimated analytically from resonant Carrier powers; no direct modeling of GW-induced sidebands resonating in the SRC.

Computational Needs for an Ongoing Simulation Effort

Computational Speed Limitations:

- Currently, a complete set of simulation runs (carrier & sideband, w/all optimizations) takes ~36 hours -- over 90% of it performing FFT's -- an amount of runtime that's difficult for a grad student, unacceptable for a professional scientist.
- This 36 hour figure is the fastest possible speed -- it is only true on "galahad", a Sun SPARCstation 20 with 2 cpu's, which makes it the fastest LIGO computer.
- This 36 hour figure also refers to runs with the standard gridding of 128x128. Doubling it to 256x256 (for higher resolution or a larger calculational window) increases the runtime by a factor of ~5.

RAM Limitations:

- The typical 128x128 grid run uses ~16 Megabytes of RAM to keep track of the fields & propagators. 256x256 and 512x512 grid runs therefore use 64 Mb and 256 Mb, respectively. As a result, *only galahad* can perform 256x256 runs, and *no present LIGO computer* can perform 512x512 runs.

Solutions We (Primarily Hiro, Kent & Greg) Are Looking Into:

- Obtaining hardware support and advice from the Concurrent SuperComputing Consortium (CSCC), conveniently located on the Caltech campus,
- Using the Paragon system at the CSCC, a parallelized architecture of Intel nodes,
- Buying time on a Cray Supercomputer, as was done in the past,
- Purchasing hardware (FFT box, Unix box?) to do very fast FFT's.



Some Conclusions

- The FFT Simulation Initiative begun at MIT has played an important role in the development of the First-Generation LIGO Detector,
- This role continues to evolve in scope and usefulness to the LIGO project,
- We will require more powerful computational tools to move ahead efficiently,
- We are perfectly positioned to use our FFT simulation techniques for more advanced R&D work, such as the study of Dual-Recycling interferometers with realistic configurations, dimensions, and optics.